A Theoretical Study of the Alkylation Reaction of Toluene with Methanol Catalyzed by Acidic Mordenite

Ann M. Vos,[†] Xavier Rozanska,*[,§] Robert A. Schoonheydt,[†] Rutger A. van Santen,[§] François Hutschka,[‡] and Juergen Hafner[#]

Contribution from the Katholieke Universiteit Leuven, Departement Interfasechemie, Kardinaal Mercierlaan 92 B-3001 Heverlee, Belgium, Schuit Institute of Catalysis, Laboratory of Inorganic Chemistry and Catalysis, Eindhoven University of Technology, P.O. Box 513, 5600 MB Eindhoven, The Netherlands, Département Chimie des Procédés, Centre Européen de Recherche et Technique, TotalFina, B.P. 27, 76700 Harfleur, France, and Institut für Materialphysik, Universität Wien, Sensengasse 8, A-1090 Wien, Austria

Received June 5, 2000. Revised Manuscript Received December 27, 2000

Abstract: A theoretical study of the alkylation reaction of toluene with methanol catalyzed by the acidic Mordenite (Si/Al = 23) is reported. Cluster DFT as well as periodical structure DFT calculations have been performed. Full reaction energy diagrams of the elementary reaction steps that lead to the formation of the three xylene isomers are given. The use of periodical structure calculations allows one to account for zeolite framework electrostatic contributions and steric constraints that take place in zeolitic catalysts. Especially the steric constraint energy contribution has a significant effect on the energies and bond formation paths. The activation energy barrier of *p*-xylene formation is found to be ∼20 kJ/mol lower than the corresponding values for the formation of its isomers. Computed host−guest binding energies according to the DFT method need a correction due to the absence of the dispersive interaction with the zeolite wall. Apparent activation energies obtained with this correction are in good agreement with experimental data.

1. Introduction

Zeolites can be used as catalysts among others for the conversion of aromatics.[1] Electrophilic aromatic substitution, one of the reactions that we will discuss, can be carried out by a variety of reactants such as olefins, alcohols, and halogenated hydrocarbons.[2] If methanol is used for the toluene alkylation over ZSM-5, selectivity for *p*-xylene of almost 100% is possible.[3]

The observed selectivity partially originates from ZSM-5's specific pore size, which imposes steric limitations on the guest molecules.[4] Treatment of ZSM-5 with phosphoric acid reduces the pore size of the catalyst channel and thus increases the *para* isomer selectivity.[3] Restrictions on the size of the transition state (transition state shape selectivity) inhibit polyalkylation, and the preferential desorption of products with high diffusivity (product shape selectivity) also enhances the yield of the *para* isomer.

For large pore zeolites such as Mordenite, the *para* selectivity is less pronounced.[5]

Not only the structure of the zeolite but also its chemical composition (e.g. Al content) influences the selectivity. The *para* selectivity over large pore zeolites is slightly enhanced when the strength of the acid sites increases.[2,6]

In general, the observed selectivity can be attributed to a combination of differences in (i) diffusivity, (ii) adsorption behavior, and (iii) intrinsic reaction rate of the xylene isomers.[7] Whereas diffusivity and adsorption behavior may be better described by using classical dynamic or Monte Carlo simulations,[8] quantum-chemical calculations offer the opportunity to study reactivity.

Despite the fact that an explanation of the reaction mechanism for the alkylation of aromatics is not only of fundamental interest and can also help to optimize reaction conditions and to find better catalysts for the reaction, full details of the reaction mechanism are not yet known.

The actual carbon−carbon bond formation in the alkylation of benzene or toluene can proceed in consecutive reaction steps or via an associative reaction mechanism.[9]

Until some time ago, it was generally accepted that the

* Address correspondence to this author. Fax +31 40 245 5054. E-mail: tgakxr@chem.tue.nl.
[†] Katholieke Universiteit Leuven.
[§] Schuit Institute of Catalysis.
[‡] Centre Européen de Recherche et Technique, TotalFina.
[#] Universität Wien.

(1) Venuto, P. B. *Microporous Mater.* **1994**, *2*, 297−411.
(2) Venuto, P. B.; Hamilton, L. A.; Landis, P. S.; Wise, J. J. *J. Catal.* **1966**, *4*, 81−98.
(3) (a) Chen, N. Y.; Kaeding, W. W.; Dwyer, G. G. *J. Am. Chem. Soc.* **1979**, *101*, 6783−6784. (b) Keading, W. W.; Chu, C.; Young, L. B.; Weinstein, B.; Butter, S. A. *J. Catal.* **1981**, *67*, 159−174.
(4) (a) Csiscery, S. M. *Zeolites* **1984**, *4*, 202−213. (b) Weisz, P. B. *Pure Appl. Chem.* **1980**, *52*, 2091−2103. (c) Ribeiro, F. R.; Alvarez, F.; Henriques, C.; Lemaos, F.; Lopes, J. M.; Ribeiro, M. F. *J. Mol. Catal. A* **1995**, *96*, 245−270.
(5) Martens, J. A.; Perez-Pariente, J.; Sastre, E.; Corma, A.; Jacobs, P. A. *Appl. Catal.* **1988**, *45*, 85−101.
(6) (a) Yashima, T.; Ahamed, H.; Yamazaki, K.; Katsuka, M.; Hara, N. *J. Catal.* **1970**, *16*, 273−280. (b) Yashima, T.; Ahamed, H.; Yamazaki, K.; Katsuka, M.; Hara, N. *J. Catal.* **1970**, *17*, 151−156.
(7) Wang, J. G.; Li, Y. W.; Chen, S. Y.; Peng, S. Y. *Zeolites* **1995**, *15*, 288−292.
(8) (a) Kiselev, A. V.; Quang Du, P. *J. Chem. Soc., Faraday Trans. 2* **1981**, *77*, 1−15. (b) Smit, B.; Siepmann, J. I. *J. Chem. Phys.* **1994**, *98*, 8442−8452. (c) Smit, B. *Mol. Phys.* **1995**, *85*, 153−172.
(9) (a) Blaszkowski, S. R.; Van Santen, R. A. *Transition State Modeling for Catalysis*; Truhlar, D. G., Morokuma, K., Eds.; ACS Symp. Ser. No. 721; American Chemical Society: Washington, DC, 1999; Chapter 24. (b) Ivanova, I. I.; Corma, A. *J. Phys. Chem. B* **1997**, *101*, 547−551.

10.1021/ja001981i CCC: $20.00
Published on Web 03/02/2001

alkylation of aromatics over acid zeolites proceeds via methoxy intermediate formation.[10] The methoxy intermediate can be generated by dissociation of methanol over an acid site resulting in water and a methyl group bound to a lattice oxygen. Proof for the existence of such alkoxy species inside zeolites can be found in experimental studies: (i) IR frequencies of 2980 to 2977 cm^{-1} are assigned to the asymmetric CH_3 stretch vibration in alkoxy species[11] and (ii) ^{13}C NMR studies reveal a chemical shift of 53 to 59 ppm for the alkoxy carbon.[12] Furthermore, theoretical calculations indicate that the alkoxy species are local minima and thus stable intermediates.[13]

The other possible reaction mechanism is the associative reaction that proceeds via coadsorption of the aromatic and methanol. Ivanova et al. performed in situ ^{13}C MAS NMR experiments during toluene alkylation with methanol.[9b] Methoxy species were found to be very stable under reaction conditions and not very reactive. The methanol species that adsorb in a way that the hydroxyl of methanol interacts with the zeolite acid site (end-on adsorption complexes) are found to be more reactive. Cluster-based calculations confirm that the associative mechanism circumventing alkoxy formation is more favorable.[9a]

Cluster calculations are very useful for the study of zeolite-catalyzed reactions.[14] They give a qualitative estimate of activation energies and can predict the favorable mechanisms. However, theoretical investigations of the electrophilic aromatic substitution are rare.

Beck et al. used Density Functional Theory (DFT) calculations on a cluster model to investigate the H/D -exchange of benzene, the most simple electrophilic aromatic substitution reaction.[15] They found a symmetric transition state and a one-step concerted mechanism. The activation energy of 86.2 kJ/mol agrees well with experimental values obtained by ^1H MAS NMR.

Corma et al. used the Hard Soft Acid Base (HSAB) theory of Pearson to explain differences in selectivity in *ortho*/*para* alkylation of toluene when the chemical composition of the zeolite changes.[16] They started from the assumption that an intermediate methoxy species was formed. They also performed a semiempirical theoretical study of this reaction using the cluster approach method.[17]

However, a cluster is only a simplified model of the zeolite that ignores all structural and long-range influence of the zeolite lattice.[18] On the other hand, the use of a large cluster can partly allow for consideration of the zeolite lattice.[14b,19]

Additional information on the influence of the zeolite can be obtained by embedding the quantum chemical cluster in a classical potential that describes the interactions with the zeolite framework.[20] The force field used in the molecular mechanics part and the method for coupling the quantum chemical and the molecular mechanics part determine the quality of this method.

Quantum-chemical periodic structure calculations have the advantage of not requiring such embedding approaches. The quantum-chemical periodic structure codes have become of even more interest, since recently it has become possible to localize approximate transition structures.[21]

Several groups investigated the effect of embedding cluster geometries for transition states or charged species.[20b,22] It has been shown that the zeolite framework stabilization of carbonium or carbenium ion type transition states or intermediates is mainly of electrostatic short-range nature due to the charge screening effect of the zeolite framework. The embedding of transition states leads to a decrease of the activation energy by 20 to 50% compared with cluster results.

Since the periodical quantum mechanical method is based on DFT methods, the van der Waals interaction is not properly computed.[23] This is a severe problem, since the interaction of aromatic adsorbates with the zeolite wall depends sensitively on this contribution.[24] We will employ an approximate energy correction scheme to overcome this shortcoming of the DFT method.

In this work the associative mechanism for the methylation of toluene with methanol over acidic Mordenite[25] (H-MOR) type zeolite will be studied.

Toluene can be alkylated in the *ortho*, *meta*, or *para* positions of the methyl substituent. For each reaction product three

(10) (a) Kazansky, V. B. *Stud. Surf. Sci. Catal*. **1994**, *85*, 251−272. (b) Corma, A.; Sastre, G.; Viruela, P. *Stud. Surf. Sci. Catal*. **1994**, *84*, 2171−2178.

(11) Kubvelkova, L.; Novakova, J.; Nedomova, K. *J. Catal*. **1990**, *124*, 441−450.

(12) Bosacek, V. *J. Phys. Chem.* **1993**, *97*, 10732−10737.

(13) (a) Kazansky, V. B.; Senchenya, I. N. *J. Catal.* **1989**, *119*, 108−120. (b) Kazansky, V. B. *Catal. Today* **1999**, *51*, 419−434.

(14) (a) Van Santen, R. A.; Kramer, G. J. *Chem. Rev.* **1995**, *3*, 637−660. (b) Frash, M. V.; Van Santen, R. A. *Top. Catal.* **1999**, *9*, 191−205.

(15) Beck, L. W.; Xu, T.; Nicholas, J. B.; Haw, J. F. *J. Am. Chem. Soc.* **1995**, *117*, 11594−11595.

(16) Corma, A.; Llopis, F.; Viruela, P.; Zicovich-Wilson, C. *J. Am. Chem. Soc.* **1994**, *116*, 134−142.

(17) Corma, A.; Sastre, G.; Viruella, P. M. *J. Mol. Catal. A* **1995**, *100*, 75−85.

(18) (a) Sauer, J. *Cluster Models for Surface and Bulk Phenomena*; Pacchioni, G., Bagus, P. S., Parmigiani, F., Eds.; Plenum Press: New York, 1992; p 533. (b) Van Santen, R. A. *J. Mol. Catal. A* **1997**, *115*, 405−419. (c) Van Santen, R. A. *Catal. Today* **1997**, *30*, 377−389. (d) Sherwood, P.; de Vries, A. H.; Collins, S. J.; Greatbanks, S. P.; Burton, N. A.; Vincent, M. A.; Hillier, I. H. *Faraday Discuss.* **1997**, *106*, 79−92.

(19) (a) Curtiss, L. A.; Brand, H.; Nicholas, J. B.; Iton, L. E. *Chem. Phys. Lett.* **1984**, *184*, 215−220. (b) Brand, H. V.; Curtiss, L. A.; Iton, L. E. *J. Phys. Chem.* **1992**, *96*, 7725−7732. (c) Van Santen, R. A.; Kramer, G. J. *Chem. Rev.* **1995**, *95*, 637−660. (d) Blaszkowski, S. R.; Van Santen, R. A. *J. Phys. Chem.* **1995**, *99*, 11728−11738. (e) Blaszkowski, S. R.; Nascimento, M. A. C.; Van Santen, R. A. *J. Phys. Chem.* **1996**, *100*, 3463−3472. (f) Gale, J. D. *Top. Catal.* **1996**, *3*, 169−194. (g) Sauer, J.; Eichler, U.; Schäfer, A.; Von Arnim, M.; Ahlrichs, R. *Chem. Phys. Lett.* **1999**, *308*, 147−154. (h) Zygmunt, S. A.; Curtiss, L. A.; Zapol, P.; Iton, L. E. *J. Phys. Chem. B* **2000**, *104*, 1944−1949.

(20) (a) Sinclair, P. E.; de Vries, A.; Sherwood, P.; Catlow, C. R. A.; Van Santen, R. A. *J. Chem. Soc., Faraday Trans.* **1998**, *94*, 3401−3408. (b) Sauer, J.; Sierka, M.; Haase, F. *Transition State Modeling for Catalysis*; Truhlar, D. G., Morokuma, K., Eds; ACS Symp. Ser. No. 721; American Chemical Society: Washington, DC, 1999; pp 358−367.

(21) See for instance: Ciobîca, I. M.; Fréchard, F.; Van Santen, R. A.; Kleyn, A. W.; Hafner, J. *Chem. Phys. Lett.* **1999**, *311*, 185−192.

(22) (a) Vollmer, J. M.; Truong, T. N. *J. Phys. Chem. B* **2000**, *104*, 6308−6312. (b) Zygmunt, S. A.; Curtiss, L. A.; Zapol, P.; Iton, L. E. *J. Phys. Chem. B* **2000**, *104*, 1944−1949. (c) Gourseot, A.; Arbuznikov, A.; Vasilyev, V. *Density Functional Theory, a Bridge Between Chemistry and Physics*; Geerlings, P., De Prooft, F., Langenaeker, W., Eds.; VUBPRESS: Brussels, 1999; pp 155−168.

(23) (a) Sauer J.; Ugliengo, P.; Garrone, E.; Saunders, V. R. *Chem. Rev.* **1994**, *94*, 2095−2160. (b) Pelmenschikov, A.; Leszczynski, J. *J. Phys. Chem. B* **1999**, *103*, 6886−6890. (c) Kristyan, S.; Pulay, P. *Chem. Phys. Lett.* **1994**, *229*, 175−180. (d) Lein, M.; Dobson, J. F.; Gross, E. K. U. *J. Comput. Chem.* **1999**, *20*, 12−22.

(24) (a) Bezuz, A. A.; Kiselev, A. G.; Loptakin, A. A.; Quang Du, P. *J. Chem. Soc., Faraday Trans. 2* **1978**, *74*, 367−379. (b) Meinander, N.; Tabisz, G. C. *J. Chem. Phys.* **1983**, *79*, 416−421. (c) Bell, R. G.; Lewis, D. W.; Voigt, P.; Freeman, C. M.; Thomas, J. M.; Catlow, C. R. A. *Proceedings of the 10th International Zeolite Conference, 1994*; Weitkamp, J., Karge, H. G., Pfeifer, H., Hölderich, W., Eds.; Elsevier: Amsterdam, 1994; Part C, p 2075.

(25) (a) Next to Faujasite and ZSM-5, Mordenite (MOR) is one of the commercially most used zeolites in catalysis.[1] Among them we have chosen Mordenite because the smaller unit-cell facilitates the calculations. Mordenite has two sets of intersecting channels: large channels subscribed by 12 T-atoms that are straight and have a free diameter of 6.5 × 7.0 Å; small side pocket channels subscribed by 8 T-atoms and oriented perpendicularly to the main channel that have a free diameter of 2.6 × 5.7 Å. (b) Barrer, R. M.; White, E. A. D. *J. Chem. Soc.* **1952**, *2*, 1561−1571. (c) Meier, W. M. *Z. Kristallogr.* **1961**, *115*, 439−450. (d) Rouse, R. C.; Peacor, D. R. *Am. Miner.* **1994**, *79*, 175−184.

different geometries for adsorbed reactants, transition states, and adsorbed products are optimized.

Calculations with the cluster approach were done to assist input transition state geometry choices of the periodical structure calculations

2. Method

Cluster Approach. Within the cluster approach, the catalytic active site model is a small neutral zeolite fragment, terminated with hydrogen atoms or hydroxyl groups. This cluster aims to represent the Brønsted acid site in interaction with toluene, xylenes, water, methanol, or reaction intermediates. Such a methodology has been extensively used to study reactions where proton activation is involved.[9b,13−20,26] No constraints have been used for the cluster and the molecules in interaction with the cluster, as recommended before.[14,20,27] A cluster consisting of four tetrahedra ($Al(OSiH_3)_2(OHSiH_3)(OH)$, T_4) has been chosen. This cluster presents three electronically equivalent oxygen atoms that are used to model the catalytic active sites.

Cluster calculations have been performed with *Gaussian98*[28] using the 6-31g* basis set[29] and the density functional method with the Perdew-Wang 1991 exchange functional as modified by Adamo and Barone[30] and the Perdew and Wang gradient-corrected correlation functional (MPWPW91).[31]

Geometry optimization calculations have been carried out to obtain a local minimum for reactants, adsorption complexes, and products and to determine the saddle point for transition states (TS). The frequencies were computed by using analytical second derivatives to check that the stationary point found exhibits the proper number of imaginary frequencies: none for a minimum and one for a transition state (first-order saddle point). Zero point energy (ZPE) corrections have been calculated for all optimized structures.

Periodical Approach. Periodical ab initio calculations have been performed by using the Vienna Ab Initio Simulation Package (VASP).[32] The total energy is calculated by solving the Kohn−Sham equations, using the exchange-correlation functional proposed by Perdew and Zunger.[33] Results are corrected for nonlocality in the generalized gradient approximation with the Perdew Wang 91 functional.[34] VASP uses plane waves and ultrasoft pseudopotentials provided by Kresse and Hafner,[35] allowing a significant reduction of the number of plane waves. For the calculations, a cutoff of 300 eV and a Brillouin-zone sampling restricted to the Γ-point have been used. The augmentation charges were expanded to 900 eV.

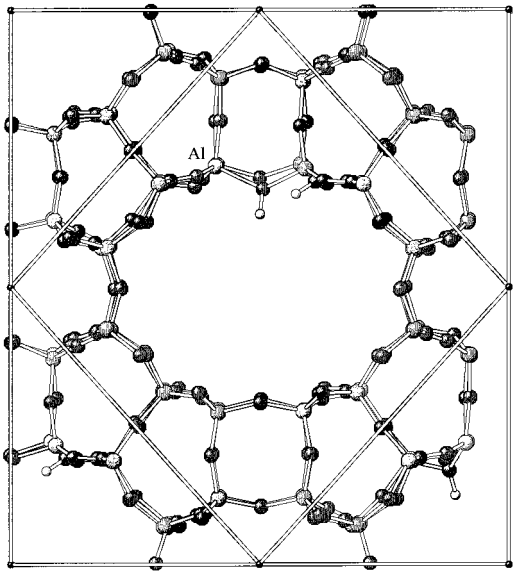

Figure 1. Mordenite unit cell. The smallest box is the unit cell that has been used in our calculations.

The zeolite structure used to perform the periodical calculations is Mordenite (see Figure 1).[25] The geometry of the unit cell of the Mordenite cell has previously been defined by using VASP by Demuth et al.[36] To avoid artificial interactions of the molecules, the minimal unit cell was doubled in the main channel direction. As a consequence our simulation box contains 146 atoms, with dimensions $a = 13.648$ Å, $b = 13.672$ Å, $c = 15.105$ Å, $\alpha = 96.792°$, $\beta = 90.003°$, and $\gamma = 90.022°$, whereas dimensions of the nonmodified Mordenite unit cell are $a = 18.14$ Å, $b = 20.43$ Å, and $c = 7.55$ Å, in good agreement with other theoretical studies.[37] The unit cell contains two Brønsted acidic sites. The acidic site positions have been selected at the junction of 12- and 8-membered rings. Demuth et al.[36] and Sauer et al.[37] have shown in their theoretical studies that aluminum atoms in these positions are the most stable for this zeolite. The position of the proton is of less importance due to its relatively high mobility.[20b,38] Relaxation of adsorbed compounds and intermediates has been done employing a quasi-Newton algorithm based on the minimization of analytical forces. Convergence has been considered to be achieved when forces on the unit cell atoms were less than 0.07 eV/Å. Our system, the Mordenite unit cell, methanol, and toluene, consists of 167 atoms.

The VASP transition state search method employed was the nudged elastic band method (NEB).[39] The transition state system geometry images were only allowed to move into the direction perpendicular to the current hypertangent, defined as the normal vector between the neighboring images. In this study the initial number of images was 8. This number was reduced to the fourth closer geometry to the maximum of energy after several steps when the transition state geometry was more clearly defined. Finally, when only a few atoms presented forces above the convergence criteria, a quasi-Newton algorithm relaxation based on force minimization was performed on the highest energy image to speed up convergence and to release transition state geometry from constraints due to the elastic band. Due to the knowledge of the transition state geometries from the cluster approach results and also due to the complexity of the mechanisms involved, the initial image geometries were not defined by automatic linear interpolation between product and reactant but adapted from the cluster calculation transition

(26) (a) Kramer, G. J.; de Man, A. J. M.; Van Santen, R. A. *J. Am. Chem. Soc*. **1991**, *113*, 6435−6441. (b) Kramer, G. J.; Van Santen, R. A. *J. Am. Chem. Soc*. **1993**, *115*, 2887−2897. (c) Rigby, A. M.; Kramer, G. J.; Van Santen, R. A. *J. Catal*. **1997**, *170*, 1−10.

(27) Eichler, U.; Brändle, M.; Sauer, J. *J. Phys. Chem. B* **1997**, *101*, 10035−10050.

(28) Frisch, M. J.; Trucks, G. W.; Schlegel, H. B.; Scuseria, M. A.; Robb, M. A.; Cheeseman, J. R.; Zakrzewski; Montgomery, J. A.; Stratmann, R. E.; Burant, J. C.; Dapprich, S.; Millam, J. M.; Daniels, A. D.; Kudin, K. N.; Strain, M. C.; Farkas, O.; Tomasi, J.; Barone, V.; Cossi, M.; Cammi, R.; Mennucci, B.; Pomelli, C.; Adamo, C.; Clifford, S.; Ochterski, J.; Petersson, G. A.; Ayala, P. Y.; Cui, Q.; Morokuma, K.; Malick, D. K.; Rabuck, D. K.; Raghavachari, K.; Foresman, J. B.; Cioslowski, J.; Ortiz, J. V.; Stefanov, B. B.; Liu, G.; Liashenko, A.; Piskorz, P.; Komaromi, I.; Gomperts, R.; Martin, R. L.; Fox, D. J.; Keith, T.; Al-Laham, M. A.; Peng, C. Y.; Nanayakkara, A.; Gonzales, C.; Challacombe, M.; Gill, P. M. W.; Johnson, B. G.; Chen, W.; Wong, M. W.; Andress, J. L.; Head-Gordon, M.; Replogle, E. S.; Pople, J. A. Gaussian 98 (revision A.1); Gaussian, Inc.: Pittsburgh PA, 1998.

(29) (a) Petersson, G. A.; Al-Laham, M. A. *J. Chem. Phys*. **1991**, *94*, 6081−6090. (b) Petersson, G. A.; Bennett, A.; Tensfeldt, T. G.; Al-Laham, M. A.; Shirley, W. A.; Mantzaris, J. *J. Chem. Phys*. **1988**, *89*, 2193−2218.

(30) Adamo, C.; Barone, V. *Chem. Phys. Lett*. **1997**, *274*, 242−250.

(31) (a) Perdew, J. P.; Wang, Y. *Phys. Rev. B* **1992**, *46*, 12947−12954. (b) Levy, M.; Perdew, J. P. *Phys. Rev. B* **1993**, *48*, 11638−11645. (c) Perdew, J. P.; Burke, K.; Wang, Y. *Phys. Rev. B* **1996**, *54*, 16533−16539.

(32) (a) Kresse, G.; Hafner, J. *Phys. Rev. B* **1993**, *48*, 13115−13126. (b) Kresse, G.; Hafner, J. *Phys. Rev. B* **1994**, *49*, 14251−14269. (c) Kresse, G.; Furthmüller, J. *Comput. Matter. Sci.* **1996**, *6*, 15−50. (d) Kresse, G.; Furthmüller, J. *Phys. Rev. B* **1996**, *54*, 11169−11186.

(33) Perdew, J. P.; Zunger, A. *Phys. Rev. B* **1981**, *23*, 5048−5079.

(34) Perdew, J. P.; Burke, K.; Wang, Y. *Phys. Rev. B* **1996**, *54*, 16533−16539.

(35) Kresse, G.; Hafner, J. *J. Phys. Condens. Matter*. **1994**, *6*, 8245−8257.

(36) Demuth, T.; Hafner, J.; Benco, L.; Toulhoat, H. *J. Phys. Chem. B* **2000**, *104*, 4593−4607.

(37) Brändel, M.; Sauer, J. *J. Am. Chem. Soc.* **1998**, *120*, 1556−1570.

(38) Štich, I.; Gale, J. D.; Terakura, K.; Payne, M. C. *Chem. Phys. Lett.* **1998**, *283*, 402−408.

(39) Mills, G.; Jónsson, H.; Schenter, G. K. *Surf. Sci.* **1995**, *324*, 305−337.

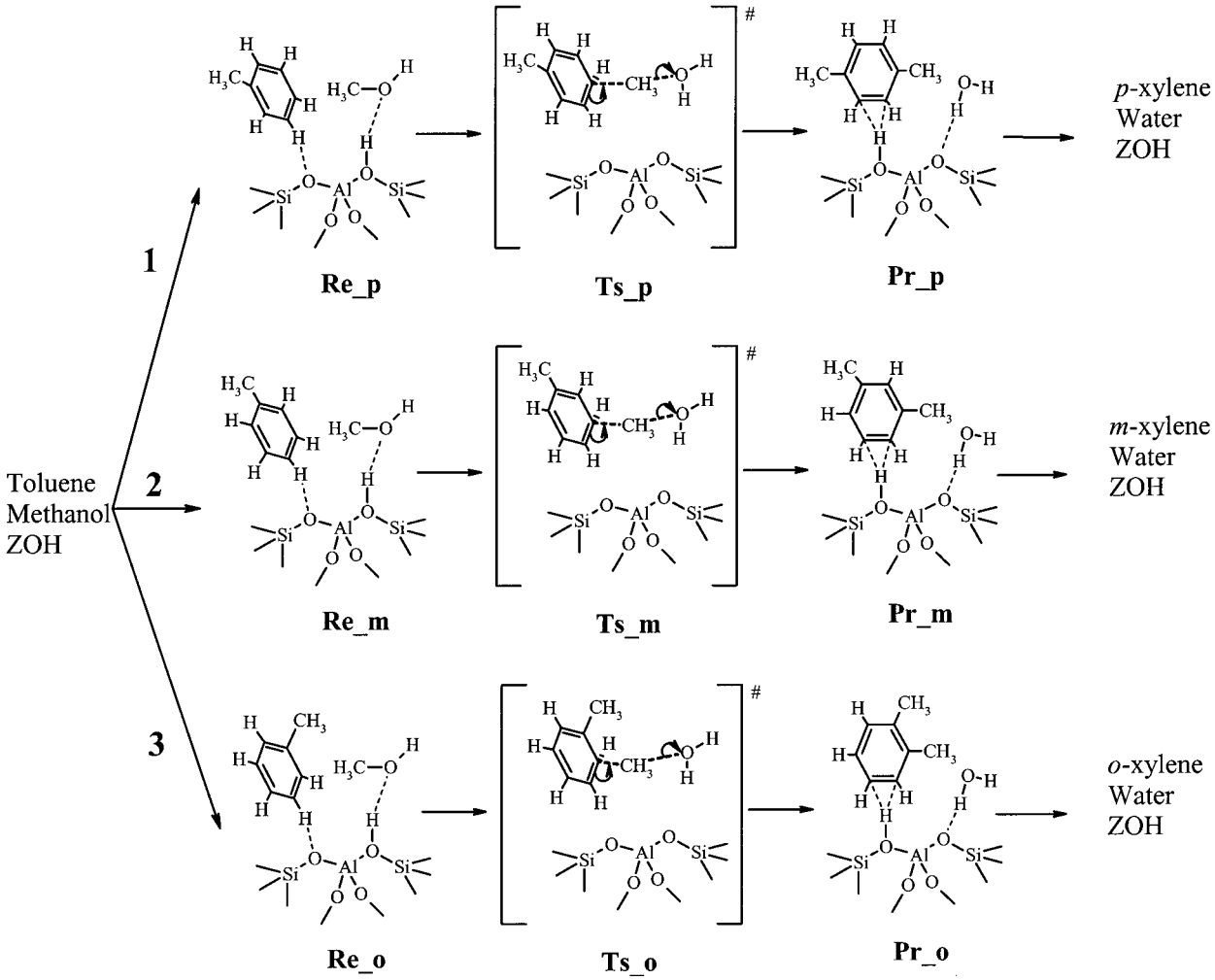

Figure 2. Mechanisms of the alkylation reaction of toluene with methanol catalyzed by acidic zeolite. The geometries between squared brackets are the geometries of the transition states as obtained from the cluster approach results (see Figure 3b).

state geometries. This approach optimizes CPU cost criteria. Cluster calculations help to validate the transition state from the periodical structure calculations, since frequency calculations of systems of sizes similar to ours are not yet possible.

van der Waals Energy Correction. DFT methods present the drawback of not properly describing the van der Waals dispersive contribution.[23] Pelmenschikov et al.[23b] have shown, using DFT and MP2 calculations, that for an aromatic species adsorbed on a neutral clay surface the dispersion contribution is of the order of ~25 kJ/mol. The Coulombic contribution was only half this value. Until now no calculations of large periodical zeolite systems at the MP2 level have been reported. Therefore a van der Waals energy correction has been applied on the toluene adsorption energy by using the parameters defined by Deka et al.[40] for aromatic species within zeolites. The expression of the computed van der Waals energy contribution is:

$$E_{\mathrm{VdW}} = \sum_{\mathrm{i,j}} \frac{(A_{\mathrm{i}}A_{\mathrm{j}})^{1/2}}{r_{\mathrm{ij}}^{12}} - \frac{(B_{\mathrm{i}}B_{\mathrm{j}})^{1/2}}{r_{\mathrm{ij}}^{6}} \qquad (1)$$

where the sum runs on i, toluene hydrogen, aliphatic carbon, or aromatic carbon, and on *j*, zeolite oxygen and silicon atoms.[40,41]

Štich et al.[42] assumed in their ab initio dynamic simulation of methanol in acidic zeolites that the dispersive contribution may not lead to modifications of the guest−host geometry. In our study we used the same assumption: the van der Waals energy contribution of the guest−host system has been evaluated by using the VASP optimized unit cell geometries. Periodic boundary conditions have been applied on the unit cell. A cutoff of 7.5 Å has been used to truncate this energy contribution. In a classical dynamic simulation of benzene and toluene within Y zeolite pores, Klein et al.[43] decomposed the guest−host energy. They showed that the van der Waals contribution remains almost constant along the minimum energy pathway and that the electrostatic contributions, mainly Coulombic, could better explain the preferred adsorption site of aromatic species in zeolites. The importance of this electrostatic interaction is enhanced when acidic sites are present.

The van der Waals correction has been applied to the periodical structure adsorption energy of toluene. Its energy and that of all consecutive intermediates and transition states have been shifted by the same value. The corrected van der Waals adsorption energy is

(40) (a) Deka, R. C.; Vetrivel, R. *J. Catal.* **1998**, *174*, 88−97. (b) Deka, R. C.; Vetrivel, R.; Miyamoto, A. *Top. Catal.* **1999**, *9*, 225−234. (c) Deka et al. defined separate parameters for zeolitic oxygen and silicon atoms and for hydrogen atom and aromatic and sp^3 carbon atoms. No parameters were defined for Brønsted acidic site aluminum atoms and acidic protons. The van der Waals contribution to the interaction between the protonic site and the guest atoms of toluene has been assumed to be the same as that for the siliceous part of the zeolite. Such approximation has been successfully used in the past.[24]

(41) In the empirical expression used repulsive and dispersive contributions cannot be decomposed as the sets of parameters A and B have been optimized in correlation. For this reason both terms in the expression have been used to correct for the dispersive interaction.

(42) Štich, I.; Gale, J. D.; Terakura, K.; Payne, M. C. *J. Am. Chem. Soc.* **1999**, *121*, 3292−12360.

(43) Klein, H.; Kirschhoch, C.; Fuess, H. *J. Phys. Chem.* **1994**, *98*, 12345−12360.

(44) (a) Schröder, K.-P.; Sauer, J.; Leslie, M.; Catlow, C. R. A.; Thomas, J. M. *Chem. Phys. Lett.* **1992**, *188*, 320−325. (b) Sauer, J. *J. Phys. Chem.* **1987**, *91*, 2315−2319.

(45) Brändel, M.; Sauer, J.; Dovesi, R.; Harrison, N. M. *J. Chem. Phys.* **1998**, *109*, 10379−10389.

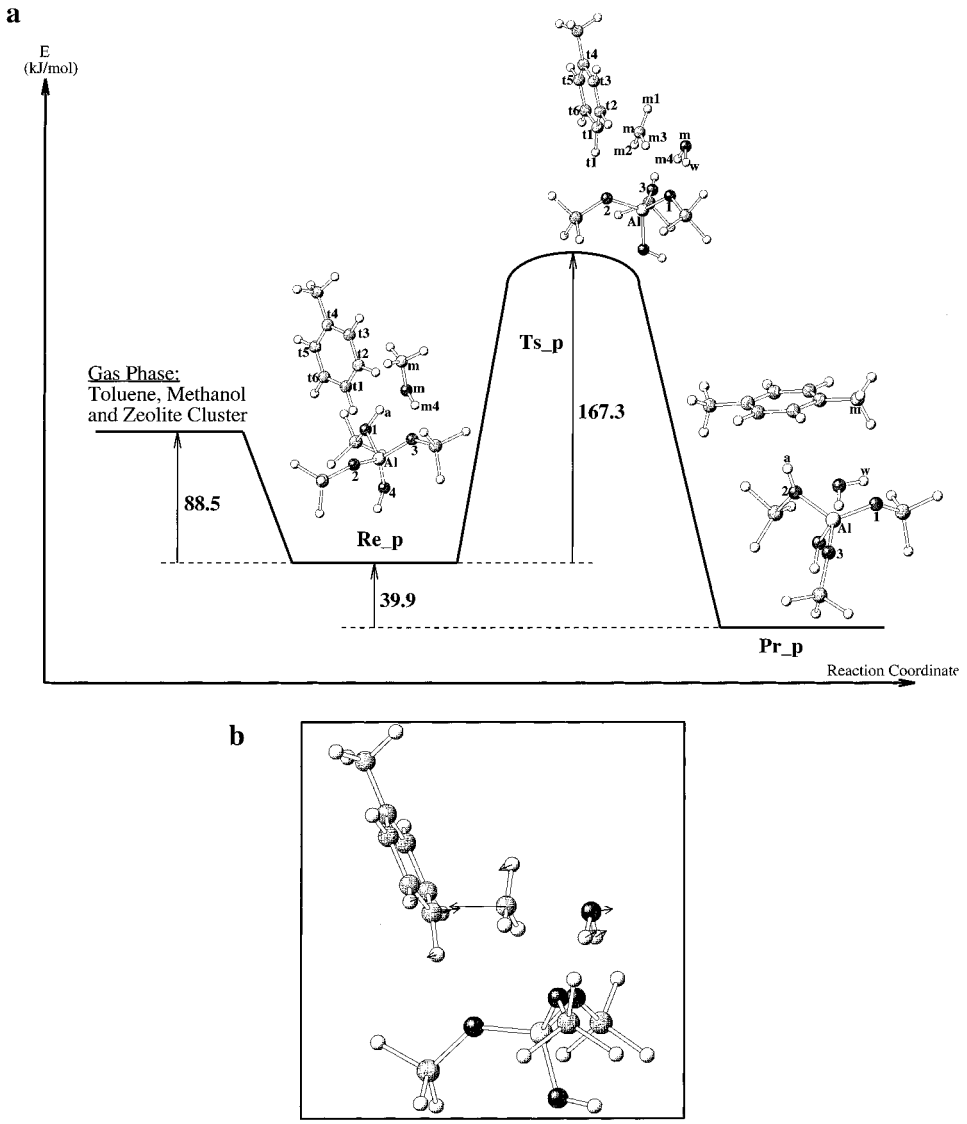

Figure 3. (a) Cluster approach reaction energy diagram and geometries of the intermediates and transition state of the alkylation reaction of toluene with methanol catalyzed by acidic zeolite leading to the formation of *p*-xylene and water. The atom labels that are used in Table 1 and geometries of the adsorbed reactants (**Re_p**), transition state (**Ts_p**), and adsorbed products (**Pr_p**) are displayed. (b) Geometry of the transition state that leads to the formation of *p*-xylene and water (**Ts_p**). The vectors are the normal mode components of the imaginary frequency of vibration.

expressed as:

$$E_{\text{ads}}^{\text{corrected}} = E_{\text{ads}} + E_{\text{VdW}} \quad (2)$$

where E_{ads} is the adsorption energy obtained by the periodic structure calculation and E_{VdW} the van der Waals energy correction according to (1). More details are provided in the discussion.

3. Results and Discussion

3.1. Cluster Approach. This part concentrates on theoretical results obtained from the cluster approach. The level of calculation, MPWPW91 in combination with the 6-31g* basis set, was chosen to make comparison possible with the periodical structure calculations. In their recent QM/MM studies Sauer et al.[44] have shown that vibrational frequencies obtained in the cluster approach are close to the corresponding QM/MM ones. They demonstrated that their QM/MM method produces results comparable to periodical calculations.[45]

The methylation of toluene is considered to proceed via an associative mechanism (see Figure 2). Toluene and methanol coadsorb on the acid site of the cluster to form an adsorption complex. This will react to form *p*-, *m*-, or *o*-xylene and water. These products have to desorb to give the final products. The energy profile of this reaction for the formation of *p*-xylene is given in Figure 3.

The optimized structure for the adsorbed reactants leading to *p*-xylene (**Re_p**) is shown in Figure 3. Differences in geometries for the intermediates that lead to formation of *meta*- and *ortho*-xylene (**Re_m** and **Re_o**) can be found in Table 1. The labels used for the atoms are shown in Figure 3.

Methanol is adsorbed in an end-on adsorption mode and is stabilized by two H-bonds with the cluster.[9a] The acid proton of the cluster is at a distance of 1.47 Å of the oxygen atom of methanol. The proton of methanol is in interaction with a bridging basic oxygen atom of the cluster (distance around 1.77 Å). Toluene is coadsorbed and the methyl of methanol is interacting with the aromatic ring.

We found three different transition structures leading to the three different products. The geometry of the transition state leading to *p*-xylene can be seen in Figure 3 (**Ts_p**) and the geometry differences between the other transition states (**Ts_m**

Table 1. Geometry of the Adsorbed Reactants (**Re_p**, **Re_m**, **Re_o**), Transition State for Formation of *p*-Xylene (**Ts_p**), *m*-Xylene (**Ts_m**), and *o*-Xylene (**Ts_o**), and Adsorbed *p*-Xylene and Water (**Ads_prod**) in the Cluster Approach[a]

	Re_p	Re_m	Re_o	Ts_p	Ts_m	Ts_o	Ads_prod
OH_a	1.06	1.06	1.06	1.84	1.83	1.80	0.99
$AlOH_a$	110.0	109.8	110.3	106.4	106.5	106.4	130.9
$AlSiOH_a$	132.9	132.5	133.7	157.1	153.8	157.7	171.8
AlC_m	4.41	4.43	4.39	3.45	3.44	3.50	4.63
H_aO_m	1.47	1.47	1.47	1.00	1.00	1.00	
$H_{m4}O_3$	1.76	1.77	1.77	1.81	1.84	1.84	2.08
O_1Hw							2.09
O_mC_m	1.44	1.44	1.44	2.25	2.28	2.25	3.67
C_mCt_1	3.96	3.96	3.98	1.98	1.95	1.97	1.51
Ct_1Ht_1	1.09	1.09	1.09	1.10	1.11	1.10	2.86
Ht_1O_2	2.70	2.74	2.83	2.12	2.08	2.25	
$O_mC_mCt_1$	99.8	98.5	101.9	170.5	170.2	170.7	85.0
$Ct_4Ct_1C_m$	83.6	75.2	77.5	110.4	111.2	105.5	178.8
$H_{m1}H_{m2}H_{m3}C_m$	35.2	35.2	35.4	−14.5	−15.9	−15.1	−38.0
$Ct_2Ct_6Ct_1C_m$	87.1	78.9	82.6	111.2	111.8	109.0	178.9

[a] The names of the atoms are as indicated in Figure 3. Distances are given in Å, angles and dihedral angles in deg.

and **Ts_o** for formation of *m*- and *o*-xylene, respectively) are shown in Table 1.

In the transition state, the acid proton of the cluster becomes attached to the oxygen of methanol (the H_aO_m distance is 1.00 Å). The methyl group of methanol is moving toward toluene. The O_mC_m distance is between 2.25 and 2.28 Å, which is larger than in the case of the adsorbed reactants (1.44 Å). Moreover the methyl is not yet completely bonded to toluene. The toluene carbon atom, which the methyl group will bind, has a distance between 1.95 and 1.98 Å to the carbon atom of the methyl group. This is still larger than the 1.51 Å of the final product. The attacking methyl group is almost planar and is in a staggered conformation relative to toluene. The methyl group adopts a η^2(HH) configuration with the Lewis basic oxygen atoms.

The toluene proton that after methylation will be given back to the cluster has not moved much yet: its distance from the toluene carbon atom remains almost steady (1.09 to 1.11 Å). The reason of this is clarified in Figure 3b. This figure displays the normal mode components corresponding to the imaginary frequency of vibration of the transition state. It can be seen that protonation of methanol and proton back-donation to the zeolitic cluster from the aromatic species are consecutive steps.

The geometry of the products has only been calculated for formation of *p*-xylene and water and can be found in Figure 3 and Table 1. The water molecule is adsorbed by two hydrogen bonds with the basic oxygen atoms of the cluster (proton−oxygen distances are 2.09 and 2.08 Å, respectively). The oxygen atom of water is in interaction with the slightly positively charged methyl protons of *p*-xylene (O_mC_m is 3.67 Å). The *p*-xylene molecule is adsorbed on the acid site of the cluster in a η^2(CC) adsorption configuration mode.

The activation energies (E_{act}) for formation of *p*-, *m*-, and *o*-xylene with respect to the energies of adsorbed reactants are given in Table 2. As expected E_{act} of *o*-xylene formation is the lowest and E_{act} of *m*-xylene formation is the highest. Since cluster calculations do not reproduce steric constraints of the cavity, the same relative order is observed as for homogeneous reactions. The preferred positions for electrophilic substitution follow the order *ortho* > *para* > *meta*.[1]

The energy difference between the adsorbed reactants and the adsorbed products (ΔE_{p-r}) is − 39.9 kJ/mol for the formation of *p*-xylene. According to the calculation, the adsorption enthalpy for methanol and toluene coadsorbed on the acid cluster (ΔH_{ads}) is around −86 kJ/mol (see Table 2).

To get better insight into the influence of the zeolite lattice on the adsorbed molecules as well on the transition states itself, periodical crystal calculations are necessary.

Table 2. Adsorption Energies and Activation Barrier Energies[a]

(a) Adsorption Energies of Toluene and Methanol within the Cluster Approach (in kJ/mol)

	Re_p	Re_m	Re_o
E_{ads}	−88.5	−88.8	−89.3
$\Delta_{298}H_{ads}$	−85.42	−87.85	−86.20
$\Delta_{298}G_{ads}$	−5.24	−2.26	−3.30
$\Delta_{298}S_{ads}$	−268.9	−287.1	−278.0

(b) Activation Barrier Energies for Alkylation Reaction of Toluene by Methanol within the Cluster Approach (in kJ/mol)

	Ts_p	Ts_m	Ts_o
E_{act}	167.3	173.2	164.4
$\Delta_{298}H^{\#}$	162.20	172.47	161.89
$\Delta_{298}G^{\#}$	190.05	187.75	178.23
$\Delta_{298}S^{\#}$	−93.4	-51.2	−54.8

[a] E_{act} values are zero-point corrected energies. Other data are calculated for a temperature of 298.15 K.

3.2. Periodical Approach. (a) Adsorption of Reactants. The first part of this report on results obtained with periodical structures focuses on the adsorption of the reactants. A variety of adsorption modes exist inside the zeolite micropore. The local minima for adsorption modes that are geometrically close to the transition states are quite different from each other dependent on whether *p*-, *m*-, or *o*-xylene will be formed (see **Ads_p**, **Ads_m**, and **Ads_o**, respectively in Figure 4).

In an IR spectroscopy study of alkylation of toluene by methanol within acidic ZSM-5 zeolite, Lercher et al.[46] demonstrated that toluene and methanol are present as an associated complex. Toluene is proposed to be in interaction with the hydrogen atom of the alcohol group, while methanol is strongly adsorbed via the oxygen atom to the acidic site proton. The initial adsorption geometry of methanol and toluene, **Co_ads**, has been taken similar to this experimental result (see Figure 5). This geometry corresponds to the global minimum of this system.

The position of the zeolitic Al connected via O to the proton that will catalyze the reaction has been chosen at the intersection of the 12- and 8-ring channel. The acid proton points inside the 12-ring channel. Upon interaction with an adsorbing molecule the geometry of the acid site will change. Before adsorption, the O_1H_a distance is 0.98 Å. The AlO_x distance is

(46) (a) Mirth, G.; Lercher, J. A. *J. Phys. Chem.* **1991**, *95*, 3736−3740. (b) Mirth, G.; Lercher, J. A. *J. Catal.* **1994**, *147*, 199−206. (c) Rep, M.; Palomares, J. G.; Van Ommen, J. G.; Lefferts, L.; Lercher, J. A. In preparation.

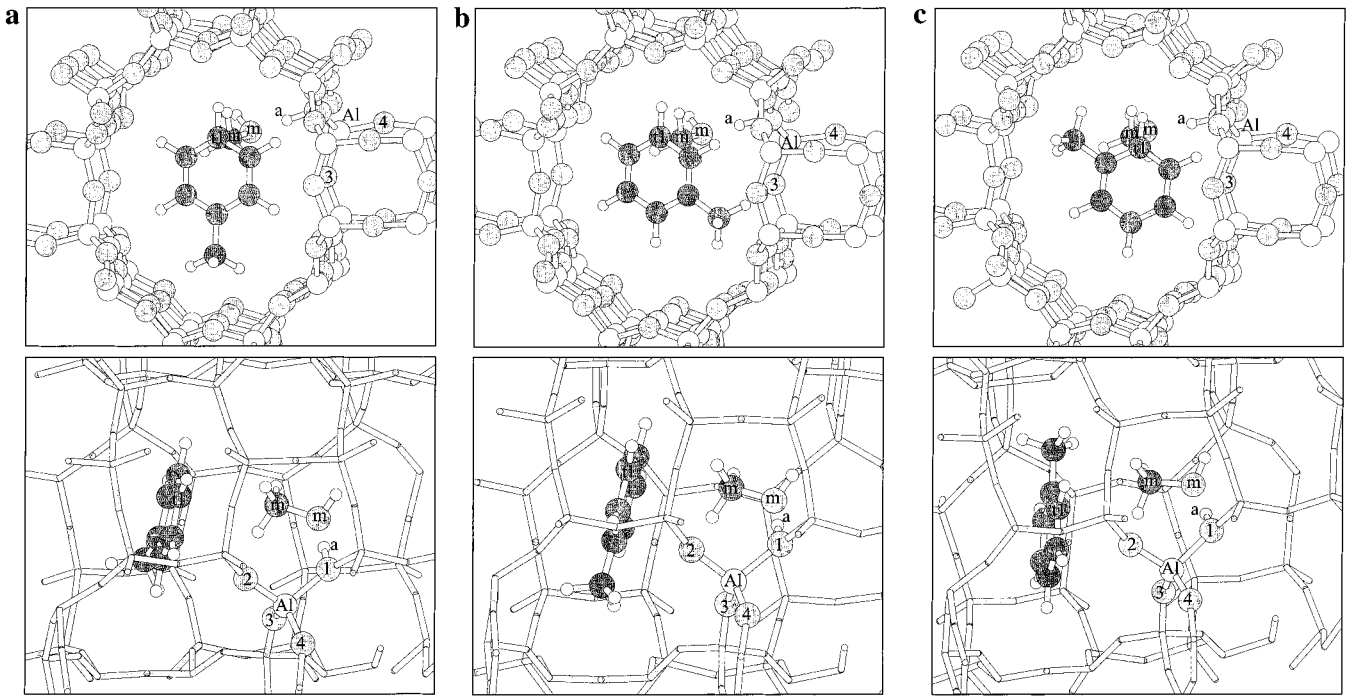

Figure 4. VASP geometries of the adsorbed reactants, toluene and methanol, within acidic Mordenite (**Ads_p** (a), **Ads_m** (b), and **Ads_o** (c), respectively). These geometries are the local minima reached by the system before the toluene alkylation reaction step.

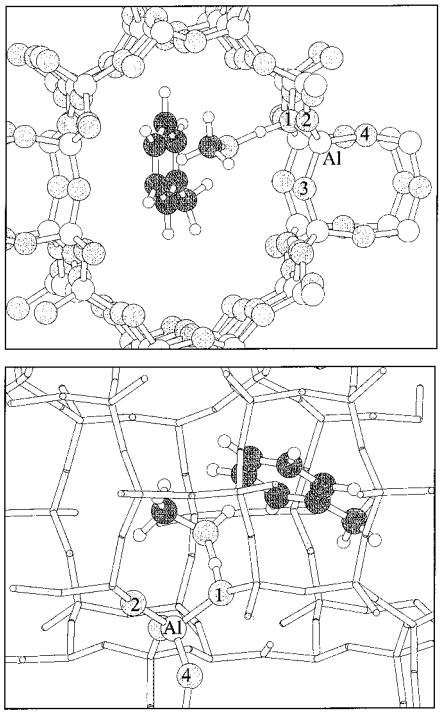

Figure 5. VASP geometry of **Co_ads**: coadsorption of toluene and methanol within acidic Mordenite.

around 1.70 Å for oxygens not connected to the acid proton ($x = 2$, 3, or 4) and 1.91 Å for the bridging hydroxyl group. After adsorption the O_1H_a bond weakens: the distance increases to around 1.09 Å for **Ads_p**, **Ads_m**, and **Ads_o**. The bond weakens even more in the case of **Co_ads** (1.14 Å), in association with a small weakening of the alcohol OH bond (0.98 to 0.99 Å). This is in agreement with the experimental data of Lercher et al.: they observed a downward shift of the alcohol IR band when toluene is added, suggesting an interaction with the alcohol proton and toluene.[46] As a result of the observed changes in O_1H_a the bonds AlO_1 and O_1Si_1 are altered as well. Furthermore, the angle and dihedral angle of the bridging hydroxyl group are also modified.

Table 3. Geometry of the Adsorbed Molecules for the Periodical Approach[a]

	Co_ads	Ads_p	Ads_m	Ads_o
H_aO_m	1.30	1.41	1.41	1.70
O_mH_m	0.99	0.97	0.98	0.98
O_mC_m	1.45	1.47	1.47	1.46
C_mCt_1		3.27	3.32	3.24
Ct_2Ht_2		1.09	1.09	1.08
Ht_2O_2		2.79	3.18	2.64
O_mH_a	1.30	1.41	1.41	1.43
$O_mC_mCt_1$		156.1	159.2	152.2
$Ct_4Ct_1C_m$		91.9	85.0	100.2
$Ct_2Ct_6Ct_1C_m$		86.5	89.2	90.2

[a] The three different adsorption states for toluene and methanol are **Ads_p**, **Ads_m**, and **Ads_o**. The names of the atoms respect the labels that have been defined in Figure 3. Distances are given in Å, angles and dihedral angles in deg.

The adsorbed molecules are located completely inside the 12-ring channel. In Table 3 some distances and angles for these molecules are given. The oxygen atom of methanol (O_m) is in close interaction with the acid proton (H_a): the H_aO_m distance is between 1.41 and 1.70 Å. In the case of **Co_ads**, this distance is even smaller ($H_aO_m = 1.30$ Å). This relates to the observed weakening of the O_1H_a bond.[46]

For **Ads_p**, **Ads_m**, and **Ads_o**, the O_mC_m bond of methanol is in the same direction as the axis of the main channel, with the methyl group pointing toward a toluene carbon (C_{t1}). The $O_mC_mC_{t1}$ angle is 152.2−159.2°. The distance between C_m of methanol and C_{t1} of toluene is around 3.3 Å. The toluene ring is positioned almost perpendicularly to the axis of the main channel. This is needed to allow the alkylation step, as was

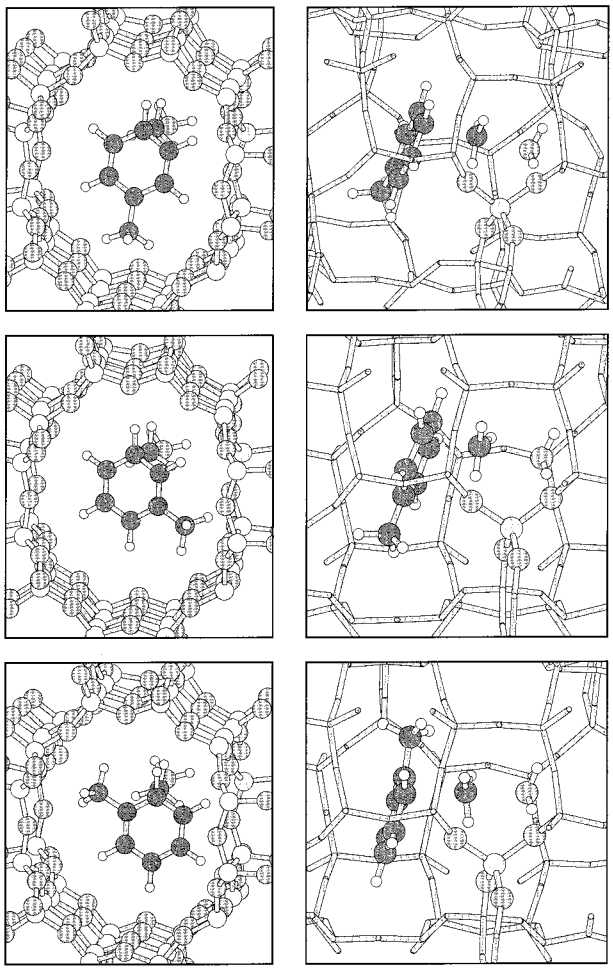

Figure 6. VASP geometries of the transition states that lead from toluene and methanol to the formation of xylene and water (from top to bottom: **Ts_p**, **Ts_m**, and **Ts_o**).

calculated from the transition states structures in the cluster study. The $C_{t4}C_{t1}C_m$ angle is around 90°. This position gives rise to interactions between the toluene hydrogen atoms and the framework oxygen atoms (see Figure 5).

Co_ads is the most stable geometry due to the strong interaction between methanol and toluene ($E_{ads} = -101.3$ kJ/mol). Aromatic species prefer to position their ring in coplanar orientation with respect to the zeolitic wall.[40,43,47] **Ads_p** is more stable than **Ads_m** and **Ads_o** with $E_{ads} = -67.5$ kJ/mol. For **Ads_m** and **Ads_o**, E_{ads} are -50.0 and -49.1 kJ/mol, respectively, due to larger steric hindrance of toluene.

(b) Transition States. For the three alkylation reaction modes, two different orientations of the attacking methyl group have been studied. From cluster results it appears that the methyl group adopts a η^2(HH) configuration with respect to the Lewis base oxygen atoms (see Figure 3). In contrast, in the periodical structure calculations a η^1 configuration has been found to be more favorable (see Figure 6). The labels used to design the transition states that lead to the three different products are the same as the ones used in the cluster approach part.

The periodical structure calculations take into account the zeolite electrostatic contribution and steric constraint contributions and allow a full relaxation of all atoms within the unit cell. The steric constraints lead to large differences when geometries of the alkylation of toluene with methanol obtained

(47) Henson, N. J.; Cheetham, A. K.; Stockenhuber, M.; Lercher, J. A. *J. Chem. Soc., Faraday Trans.* **1998**, *94*, 3759−3768.

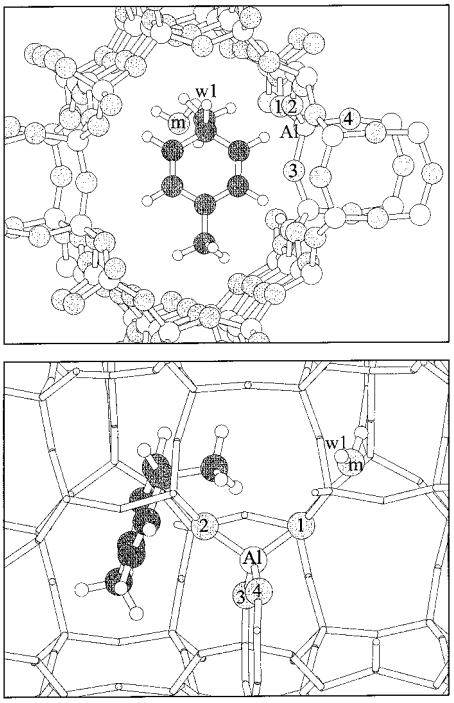

Figure 7. VASP geometry of the charged *p*-xylene and water consecutively formed after the methylation of toluene (**P_int**).

with the periodical structure approach are compared with the ones obtained with the cluster approach. In the cluster approach, a single step mechanism is found for the alkylation reaction of toluene: the Brønsted site proton attacks the methanol oxygen, followed by the jump of the methyl group between methanol and toluene, which then back-donates a proton to the cluster. In the case of the periodical structure model such a reaction pathway cannot be achieved in a single step. Protonated xylene is found to be a stable reaction intermediate, be it is activated (see **P_int** in Figure 7). A small rotational barrier has to be overcome to obtain the proper geometry for proton back-donation. It is well-known that toluene or methanol cannot exist as stable protonated species within a zeolite due to a too weak acidity of this solid acid.[48] However, experimental observations of long lifetime charged species have been obtained.[49] These are explained by zeolite steric constraints that prevent fast reorientation of the charged species[49a−c] or by the association of the charged species with other molecules.[48c,49c−g]

Another difference with the free cluster situation is found for the transition states. The hydrogen atom bonded to the toluene carbon atom that is being alkytated is not in direct interaction with a Lewis basic oxygen atom. Toluene could interact directly with a more basic oxygen atom of a Si−O−Al bridge as obtained from the cluster results. However, this results in large steric constraints if toluene keeps a favorable orientation

(48) (a) Haw, J. F.; Oshiro, I. S.; Lazo, N. D.; Speed, J. A. *J. Am. Chem. Soc.* **1989**, *111*, 2052−2058. (b) Haw, J. F.; Nicholas, J. B.; Xu, T.; Beck, L. W.; Ferguson, D. B. *Acc. Chem. Res.* **1996**, *29*, 259−267. (c) Jeanvoine, Y.; Ángyán, J. G. *J. Phys. Chem. B* **1998**, *102*, 7307−7310. (d) Paukshtis, E. A.; Malysheva, L. V.; Stepanov, V. G. *React. Kinet. Catal. Lett.* **1998**, *65*, 145−152.

(49) (a) Pazé, C.; Sazak, B.; Zecchina, A.; Dwyer, J. *J. Phys. Chem. B* **1999**, *103*, 9978−9986. (b) Bordiga, S.; Civalleri, B.; Spoto, G.; Pazé, C.; Lamberti, C.; Ugliengo, P.; Zecchina, A. *J. Chem. Soc., Faraday Trans.* **1997**, *21*, 3893−3898. (c) Auquetil, R.; Saussey, J.; Lavalley, J.-C. *Phys. Chem. Chem. Phys.* **1999**, *4*, 555−560. (d) Nicholas, J. B. *Top. Catal.* **1999**, *9*, 181−189. (e) Haw, J. F.; Xu, T.; Nicholas, J. B. *Nature* **1997**, *389*, 832−835. (f) Gorte, R. J. *Catal. Lett.* **1999**, *62*, 1−13. (g) Sárkány, J. *Appl. Catal. A* **1999**, *188*, 369−379. (h) Kazansky, V. B. *Top. Catal.* **2000**, *11−12*, 55−60.

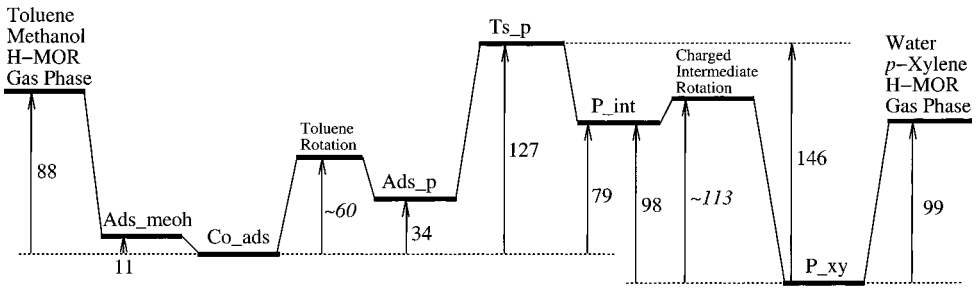

Figure 8. VASP reaction energy diagram of the reaction of alkylation of toluene with methanol catalyzed by acidic Mordenite that leads to the formation of *p*-xylene and water (all values in kJ/mol). The values correspond to energies at 0 K.

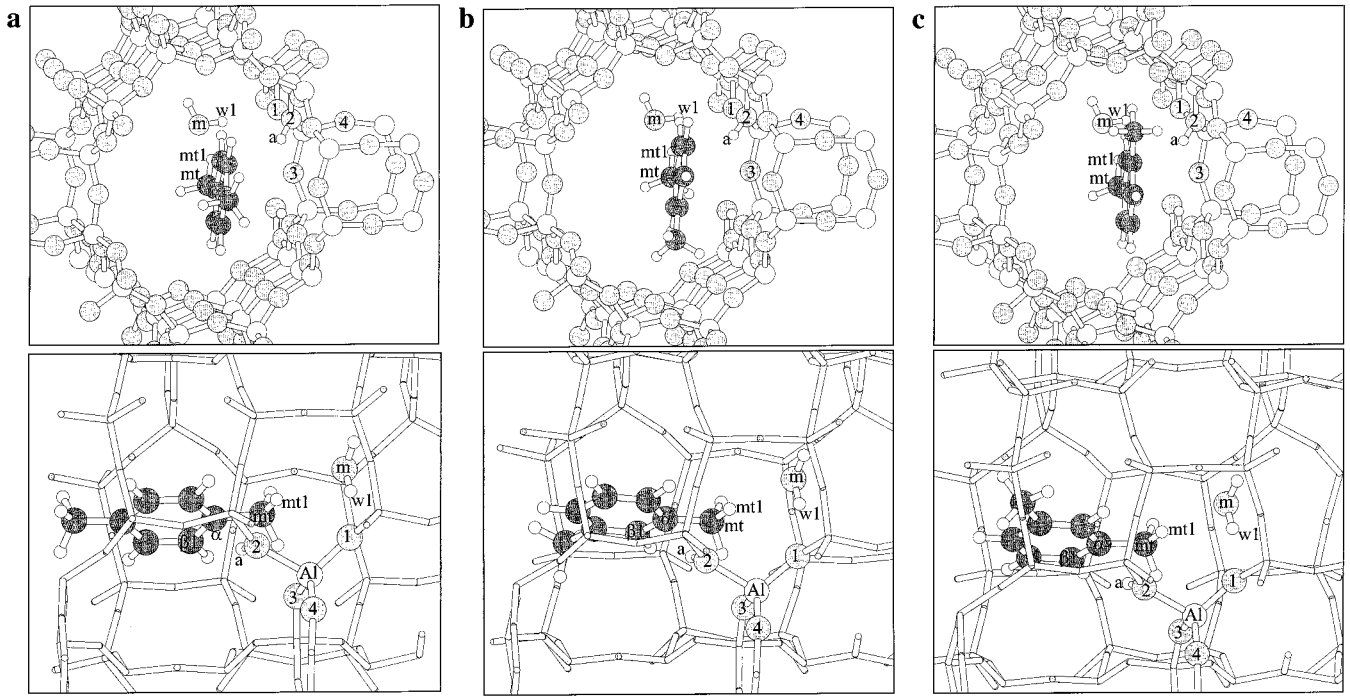

Figure 9. VASP geometries of *p*-xylene and water (a), *m*-xylene and water (b), and *o*-xylene and water (c) adsorbed within acidic Mordenite.

for the alkylation with methanol (see Figure 4). In contrast, toluene adapts its position so it increases the number of hydrogen bonds it can form with the zeolite framework oxygen atoms of Si−O−Si bridge.

In the case of the *p*-xylene formation the full reaction energy diagram has been computed (see Figure 8). The charged "pseudo" intermediate **P_int** is as one can expect less stable than both reactant and product and only ∼50 kJ/mol lower than the transition state energy level. Jobic et al.[50] reported that the activation energy barrier for the rotation around the molecular axis C_2 of benzene was between 25 and 105 kJ/mol, with an average of 60 kJ/mol, inside a 8 Å silicalite. In the case of the charged *p*-xylene one can estimate, based on these values and the energy levels of **P_int** and of water and *p*-xylene (**P_xy**), that the reorientation energy barrier should be of the order of ∼15 kJ/mol. The Polanyi−Brønsted relation has been used to obtain this number.[18b,52] This activation energy barrier is easy to overcome for the system at the temperature required to achieve this reaction. The *p*-xylene molecule reorients itself and presents its proton in excess to a Lewis base oxygen atom. Without activation barrier, the proton is back-donated to the oxygen O_2. This leads to the new configuration of the MOR unit cell. The position of the acidic proton in this MOR unit cell is slightly more favored energetically than in the initial configuration, with a $\Delta E = -14.5$ kJ/mol in good agreement with the values of Demuth et al.[36]

The lowest activation energy barrier is found for the reaction step which leads to the formation of *o*-xylene, with E_{act} equal to 92 kJ/mol. The formation of *p*-xylene and *m*-xylene corresponds to activation energy barriers 1 and 8 kJ/mol higher. These data are in agreement with the qualitative predictions of Corma et al.,[16] using the Pearson's HSAB principle. They proposed that in the absence of geometrical constraints, the Coulombic contribution preferentially directs alkylation to the *ortho* position.

(c) Adsorbed Products. After alkylation of toluene, the charged intermediate has to rotate to allow back-donation of its excess hydrogen atom to the negatively charged lattice oxygen atoms. After rotation, the back-donation mechanism occurs without activation barrier energy. The adsorption geometries and energies of the products of the three reactions have

(50) Vigné-Malder, F.; Jobic, H. *Chem. Phys. Lett.* **1990**, *169*, 31−35.
(51) According to the Polanyi−Brønsted relation, the change in activation energy is approximately proportional to the change of the energy difference between reactant and product.
(52) (a) Tsai, T.-C.; Liu, S.-B.; Wang, I. *Appl. Catal. A* **1999**, *181*, 355−398. (b) Fraenkel, D.; Levy, M. *J. Catal.* **1989**, *118*, 10−21.

Table 4. Geometries of Water and *p*-Xylene (**P_xy**), Water and *m*-Xylene (**M-xy**), Water and *o*-Xylene (**O_xy**), and Water and the Charged Aromatic Intermediate Reached after the Methylation of Toluene Prior to the Formation of *p*-Xylene (**P_int**)[a]

	P_xy	M_xy	O_xy	P_int
H_aC_α	3.38	2.93	3.15	
H_aC_{mt}	3.48	3.04	3.12	
$O_2H_aC_\alpha$	153.9	160.9	170.0	
$O_2H_aC_\alpha C_{\beta 1}$	−80.9	−77.1	−96.4	
$H_{w1}O_1$	2.25	2.21	2.23	3.28
$O_1H_{w1}O_m$	167.4	166.6	165.8	146.0
$H_{mt1}O_m$	2.42	2.31	2.57	

[a] Distances in Å, angles and dihedral angles in deg. The atom labels are displayed in Figure 9

been computed (see Figure 9 and Table 4). No geometry constraints have been used.

The geometries of adsorbed *o*-, *m*-, and *p*-xylenes in the presence of water are very similar (see Table 4). We investigated geometries that are relatively close to the geometries of the system after the proton back-donation mechanism. Water is interacting with Lewis base oxygen O_1 (H_wO_1 = 2.21 to 2.25 Å), and the proton of the acidic site is in close interaction with an aromatic ring carbon atom that binds a methyl group (C_α). The distance H_aC_α varies from 2.93 to 3.38 Å. The acidic proton interacts also with the carbon atom of the methyl group (H_aC_{mt} = 3.04 to 3.48 Å). Nevertheless H_aC_α is equal to or smaller than $H_aC_{CH_3}$. Xylene rings have been chosen coplanar with the zeolite wall as supported by classical molecular dynamic studies (see Figure 9).[40,43,47] Moreover, this orientation allows the xylene aromatic ring (via C_α) to be in interaction with the acidic proton. The oxygen atom of water is in interaction with a hydrogen atom of the methyl group ($H_{mt1}O_w$ distances between 2.31 and 2.57 Å).

The adsorption energies of *p*-xylene and water (**P_xy**), *m*-xylene and water (**M_xy**), and *o*-xylene and water (**O_xy**) are − 46.3, − 28.0, and − 19.3 kJ/mol, respectively.

The geometry of water in the three cases is very similar and differences in adsorption energies are mainly due to xylene adsorption geometries. As can be seen in Figure 9, *p*-xylene experiences the smallest steric constraint effects. In the case of *m*-xylene and *o*-xylene, the second methyl group interacts with the zeolite wall, which leads to an increase in energy. The *o*-xylene isomer experiences the largest steric constraints with an adsorption energy that is 27.0 kJ/mol less than that of *p*-xylene. The *m*-xylene adsorption energy occupies an intermediate position between the two other isomers.

3.3. Comparison with Experimental Data. Tsai et al. and Fraenkel et al. stressed that selectivity is governed by the zeolite pore structure at the reactive center.[52] Here, we have shown how steric constraints affect the course of a reaction. The alkylation reaction of toluene by methanol catalyzed by zeolite constitutes a very good illustration of transition state selectivity and has been used for this purpose for many years.[4]

A proper estimate of the adsorption energy is mandatory. Indeed the apparent experimentally measured activation energy depends on the activation energy of the rate-limiting step as well as the adsorption energy. For a first-order reaction one derives easily:

$$E_{act}^{app} = E_{act} + (1 - \theta_b)E_b^{ads} \quad (3)$$

where E_{act} stands for the activation energy of the elementary step that is rate limiting, E_{act}^{app} the apparent activation energy of the overall catalytic reaction, θ_b the coverage of a species **b** on the active site, and E_b^{ads} the adsorption energy of this species.[53] Lercher et al. reported that methanol exists in the form of a 1:1 adsorbed complex with the acidic sites, whereas a fraction of toluene adsorbs on the acidic sites,[46] supporting the assignment of **b** to the methanol−toluene coadsorbate (**Co_ads**).

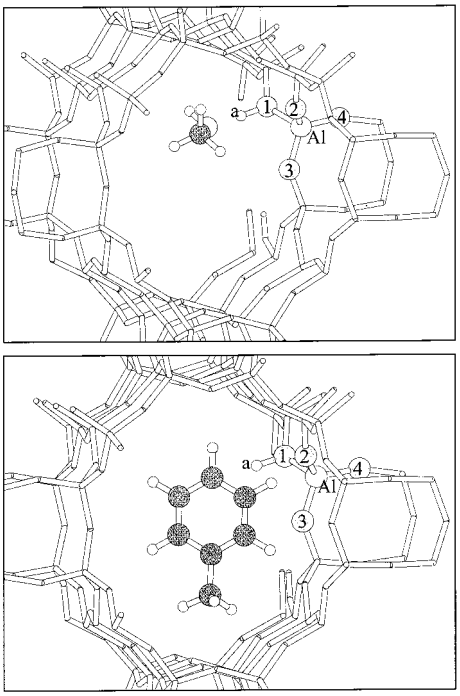

Figure 10. VASP geometry of methanol (a) and toluene (b) (using **Ads_p** toluene geometry as the input geometry) adsorbed within acidic Mordenite.

The application of (3) to our periodical results requires reliable adsorption energy values. The adsorption energies of methanol and toluene have been computed separately. The geometry of adsorbed methanol (**Ads_meoh**) is very similar to the geometry of methanol as in **Ads_**(**p**, **o**, and **m**) configurations (see Table 3 and Figure 10). **Ads_meoh** adsorption energy is in good agreement with reported experimental values (E_{ads} = − 87.9 kJ/mol),[54] without any need to include dispersion correction.[55] The geometry of adsorbed toluene has been defined using its configuration as in **Ads_p** (see **Ads_t** in Figure 10). For the periodical structure calculation, the computed adsorption energy is repulsive with +22.2 kJ/mol. Experimentally, a value of −90 kJ/mol is reported.[43] From these calculations one may deduce the interaction energy between toluene and methanol using **Ads_p** (see Table 4), **Ads_meoh**, and **Ads_t** adsorption energies. This interaction energy is about 0.9 kJ/mol. That means that toluene is not affected by the presence of methanol. Therefore the toluene and zeolite atom positions as in **Ads_p** have been used to get an evaluation of the van der Waals contribution of the toluene−zeolite guest−host system. The calculated van der Waals energy correction E_{VdW} is −52 kJ/mol. All adsorption energies are corrected by the same value using (2).

(53) (a) Haag, W. O. *Zeolites and Related Materials, State of the Art 1994*; Weitkamp, H. G., Karge, H., Pfeifer, H., Hölderich, W., Eds.; Elsevier Science: Amsterdam, 1994; pp 1375−1394. (b) Narbeshuber, T. F.; Vinek, H.; Lercher, J. A. *J. Catal.* **1995**, *157*, 388−395. (c) Van Santen, R. A.; Niemantsverdiet, J. W. *Chemical Kinetics and Catalysis*; Plenum: New York, 1995; Chapter 6.

(54) (a) Dubinin, M. M.; Rakhmatkariev, G. U.; Isirikyan, A. A. *Bull. Acad. Sci. USSR* **1989**, 2419−2421. (b) Zygmunt, S. A.; Mueller, R. M.; Curtiss, L. A.; Iton, L. E. *J. Mol. Struct.* **1998**, *430*, 9−16.

(55) Ugliengo, P.; Ferrari, A. M.; Zecchina, A.; Garrone, E. *J. Phys. Chem.* **1996**, *100*, 3632−3645.

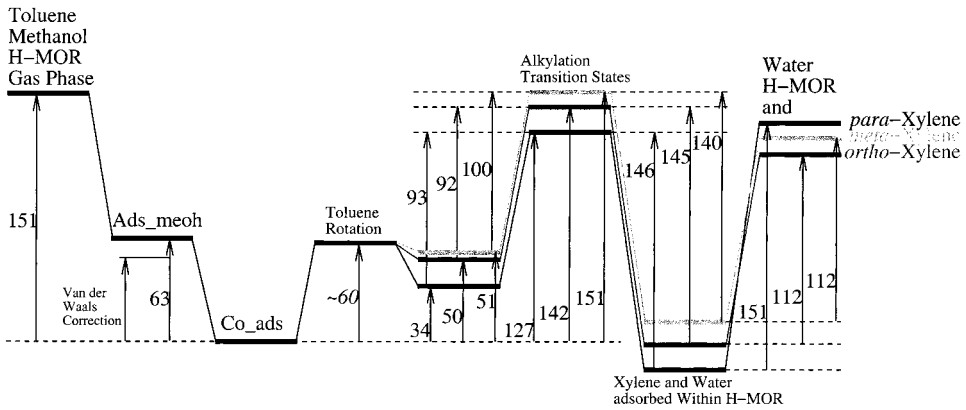

Figure 11. Dispersive energy corrected reaction energy diagram of the reactions of alkylation of toluene with methanol catalyzed by acidic Mordenite that leads to the formation of *p*-xylene, *m*-xylene, or *o*-xylene and water (all values in kJ/mol). The values correspond to energies at 0 K.

When the adsorption energy of **Co_ads** is shifted by this value its adsorption energy becomes $E_{ads}^{Co\_ads} = -151$ kJ/mol with respect to the gas phase. The decomposition of this energy into its different contributions may be expressed as:

$$E_{ads}^{Co\_ads} = E_{ads}^{meOH} + E_{ads}^{toluene} + E_{int}^{meOH-toluene} \quad (4)$$

where E_{ads}^{meOH} is the adsorption energy of methanol ($E_{ads}^{meOH} = -87.9$ kJ/mol), $E_{ads}^{toluene}$ the adsorption energy of toluene, and $E_{int}^{meOH-toluene}$ the interaction energy between toluene and methanol. Therefore $E_{ads}^{toluene}$ plus $E_{int}^{meOH-toluene}$ equals -63 kJ/mol. One may assume that $E_{int}^{meOH-toluene} \approx -10$ kJ/mol,[56] which leads to $E_{ads}^{toluene} \approx -50$ kJ/mol. This value is in reasonable agreement with the adsorption energy of toluene adsorbed within large pore zeolites.[43]

The **Co_ads** energy, which is closer to the thermodynamic minimum, has been used as a reference for the determination of activation energies of the elementary reaction step (see Figure 11).

These activation energy data relate well to experimental data.[3,16,17,46] The experimental apparent activation energy of this reaction has been reported to be ~50−90 kJ/mol.[46a] This value is in good agreement with our computed apparent activation energies when a coverage θ_b between 0.5 and 1 is assumed. However, activation energies for *p*-, *m*-, and *o*-xylene formations show large differences that issue from steric constraints. The activation energy of *p*-xylene formation is 127 kJ/mol and the activation energies of *m*- and *o*-xylene are ~20 kJ/mol above. Such activation energy differences have been reported to be large enough to explain the relatively small changes in the *para*/*ortho* selectivity observed experimentally on large pore zeolites.[17]

(56) We took $E_{int}^{MeOH-toluene}$ equal to the DFT computed value $E_{ads}^{Co\_ads} - E_{ads}^{meOH}$ (see Figure 8).

4. Conclusion

In this theoretical study, we shown how steric constraints in zeolites affect reactivity. Our results show that transition state selectivity is induced within Mordenite.[4a] Quantitatively, this selectivity can be estimated by the comparison of the activation energies: the activation energy differences are of the order of 20 kJ/mol. The order of the activation energies of xylene changes completely when the activation energies are considered in the presence and absence of steric constraints. In the absence of steric constraints the order is *ortho* < *para* < *meta*, in good agreement with the HSAB principle, whereas in the presence of steric constraints this becomes *para* < *ortho* < *meta*. These activation energy differences are not sufficient to explain the 100% selectivity shown by some catalysts. However, the pure acidic model of zeolite we used is not intended to model the modified zeolite catalysts that allow such selectivity.[3] These modified zeolite catalysts have been pre-coked and their external active sites have been deactivated. Diffusional processes may then play an important role.

The comparison with experimental activation energies requires an estimation of the adsorption energy of reactants and products. The DFT method cannot be used to compute accurately adsorption energies.[23] The guest−host binding energy in the case of the zeolite system is governed by van der Waals forces.[24] Energy correction that includes the missing van der Waals contribution leads to reasonable data that show good agreement with experimental values.

Acknowledgment. This work has been performed within the European Research Group "Ab Initio Molecular Dynamics Applied to Catalysis", supported by the Centre National de la Recherche Scientifique (CNRS), the Institut Français du Pétrole (IFP), and the TotalFina Raffinage Distributions company. Other support came from the GOA (Geconcerteerde Onderzoeksactie Vlaanderen). A.M.V. thanks the IWT for financial support. X.R. thanks TotalFina Raffinage Distributions for the financial support and Dr. Luis A. M. M. Barbosa for fruitful discussions.

JA001981I